

MAGNETOHYDRODYNAMICS USING PATH OR STREAM FUNCTIONS

YOSSI NAOR AND URI KESHET

Physics Department, Ben-Gurion University of the Negev, POB 653, Be'er-Sheva 84105, Israel

(Dated: February 28, 2019)

Draft version February 28, 2019

ABSTRACT

Non-diffusive flows can be defined by three path functions Λ_α or, for a steady flow, by two stream functions λ_κ and an auxiliary field such as the mass density ρ or the velocity v . While typical computations of a frozen magnetic field \mathbf{B} involve non-local gradients of the fluid element position $\mathbf{x}(t)$, we derive a local solution $\mathbf{B} = (\partial\mathbf{x}/\partial\Lambda_\alpha)_t \tilde{B}_\alpha \rho / \tilde{\rho}$, where Lagrangian constants denoted by a tilde are fixed at a reference hypersurface \tilde{H} on which \mathbf{B} is known. For a steady flow, this becomes $\tilde{\rho}\mathbf{B}/\rho = (\partial\mathbf{x}/\partial\lambda_\kappa)_{\Delta t} \tilde{B}_\kappa + \mathbf{v}\tilde{B}_3/\tilde{v}$, where Δt is the travel time from \tilde{H} ; here the electric field $\mathbf{E} \sim (\tilde{B}_2\nabla\lambda_1 - \tilde{B}_1\nabla\lambda_2)/\tilde{\rho}$ depends only on λ and \tilde{H} parameters. Illustrative solutions are derived for compressible axisymmetric flows and incompressible flows around a sphere, showing that viscosity and compressibility enhance the magnetization, and lead to thicker boundary layers.

Subject headings: magnetohydrodynamics (MHD) - magnetic fields - planets and satellites: magnetic fields - galaxies: magnetic fields - ISM: magnetic fields.

1. INTRODUCTION

Magnetic fields frozen in highly conductive plasmas are found in diverse astronomical systems. Examples include the solar corona, flares and wind (*e.g.*, Zhang & Low 2005; Longcope 2005), planetary magnetospheres and bow shocks (*e.g.*, Spreiter & Alksne 1970; Spreiter & Stahara 1995; Zhang et al. 2004; Corona-Romero & Gonzalez-Esparza 2013), the interstellar medium (*e.g.*, Price & Bate 2008; Li et al. 2011; Padovani et al. 2014), in particular where it meets the solar wind (Parker 1961; Aleksashov et al. 2000; Whang 2010), and the intergalactic medium of galaxy groups and galaxy clusters (Bernikov & Semenov 1979; Kim et al. 1991; Vikhlinin et al. 2001; Keshet et al. 2010; Brüggem 2013). For general reviews of magnetization in astronomical systems, see Widrow (2002); Vallée (2011).

In such systems, magnetization away from shocks and reconnection regions can be typically approximated using ideal magnetohydrodynamics (MHD), on a background ranging from a simple axisymmetric flow around a blunt object to complicated, turbulent motions. The passive evolution of magnetic fields frozen in a given flow is thus important in space physics, astrophysics, applied mathematics, and computational physics (*e.g.*, Ranger 1997; Sekhar 2003; Sekhar et al. 2005; Bennett 2008). However, present derivations of the magnetic field evolution in a general flow are inherently nonlocal.

Formally, the ideal MHD equations can be solved to give (Elsasser 1956)

$$\mathbf{B} = \frac{\rho}{\tilde{\rho}} \left(\tilde{\mathbf{B}} \cdot \tilde{\nabla} \right) \mathbf{x}, \quad (1)$$

where \mathbf{B} is the magnetic field, ρ is the mass density, \mathbf{x} is the position of the fluid element, and a tilde denotes (henceforth) a Lagrangian constant evaluated on a reference hypersurface \tilde{H} , on which \mathbf{B} is known. Thus, $\tilde{\nabla}$ is a non-local operator, acting in the vicinity of \tilde{H} , rather

than around \mathbf{x} . Therefore, to derive \mathbf{B} from Eq. (1), one must essentially integrate first over the flow to compute the mapping of \mathbf{x} on \tilde{H} .

Here we show that \mathbf{B} can be locally and simply computed using the path functions or stream functions, often used to describe the flow. Such functions exist as long as particle diffusion can be neglected (Yih 1957). Thus, time dependent flows can be fully described by three path functions, $\Lambda_{\alpha=1,2,3}$ (Yih 1957, in three spatial dimensions; henceforth). Steady flows can be fully described by two stream functions, $\lambda_{\kappa=1,2}$, which fix the mass flux $\mathbf{j} \equiv \rho\mathbf{v}$ (Giese 1951), and an additional quantity such as ρ , the velocity v , or the travel time Δt . Path (stream) functions are useful in picturing the flow, because their equi-value surfaces intersect at pathlines (streamlines), the trajectories of fluid elements in spacetime (in space).

For simplicity, we focus on non-relativistic flows, with negligible particle diffusion, in the ideal MHD limit. Arbitrary flows are considered, including those involving discontinuity surfaces such as shocks. Path (stream) functions are in general not continuous across such surfaces (*e.g.*, Giese 1951), which may also involve important kinetic plasma effects. Here, our analysis may be piecewise applied to the regions between the surfaces describing \tilde{H} and the discontinuities in the flow.

The local solution we derive for passive magnetization is analyzed for a general steady, axisymmetric flow, tested for an arbitrary time dependent, one dimensional flow, and illustrated for basic flow patterns, in particular steady flows around blunt objects used to model astronomical systems. The results indicate that passive magnetization is in general enhanced by viscosity and compressibility effects, leading to stronger magnetization in front of moving objects, and thus to thicker boundary layers.

Analytic solutions to the nonmagnetized flow around an obstacle are available only for a handful of time-independent cases, such as incompressible, potential flows around simple objects (*e.g.*, Landau & Lifshitz

1959; Leal 2007), or the approximate, compressible flow in front of an axisymmetric body (Keshet & Naor 2014). Solutions to the induced magnetization are even more rare, notable examples including the steady, incompressible, potential flow around a sphere (Chacko & Hassam 1997; Lyutikov 2006; Dursi & Pfrommer 2008; Romanelli et al. 2014) or around simplified surfaces representing for example bow shocks (Corona-Romero & Gonzalez-Esparza 2013) or the heliopause (Röken et al. 2014). We are unaware of a previous magnetization solution even for the simple, Stokes (creeping) incompressible steady flow around a sphere. Such solutions are derived as special cases of our general axisymmetric result.

The paper is organized as follows. In §2, we derive the temporal evolution of the magnetic field, for both steady and time dependent flows. Arbitrary axisymmetric flows are analyzed in §3, focusing in particular on the axis of symmetry. In §4, we present some basic flows and analyze their magnetization. The results are summarized and discussed in §5.

2. EVOLVING ELECTROMAGNETIC FIELDS

We begin in §2.1 by introducing the MHD equations, and switching to a Lagrangian perspective. Next, we analyze the evolution of \mathbf{B} for arbitrary steady (in §2.2) and time-dependent (in §2.3) flows. To demonstrate the consistency of these two frameworks, in §2.4, an arbitrary steady flow is analyzed using the time-dependent formalism.

2.1. Two viewpoints of the relation $\mathbf{B} \propto \rho \mathbf{l}$

Let \mathbf{l} be an infinitesimal vector adjoining nearby fluid elements that lie on the same magnetic field line (henceforth: length element). The magnetic field can be shown to evolve in proportion to $\rho \mathbf{l}$ (*e.g.*, Landau & Lifshitz 1960). We derive this relation in an Eulerian picture in §2.1.1, and in a Lagrangian framework in §2.1.2.

2.1.1. Eulerian picture

The ideal MHD equations,

$$\text{Gauss' law,} \quad \nabla \cdot \mathbf{B} = 0 ; \quad (2)$$

$$\text{continuity,} \quad \frac{\partial \rho}{\partial t} + \nabla \cdot (\rho \mathbf{v}) = 0 ; \quad (3)$$

$$\text{convection,} \quad \frac{\partial \mathbf{B}}{\partial t} = \nabla \times (\mathbf{v} \times \mathbf{B}) ; \quad (4)$$

$$\text{and Ohm's law,} \quad \mathbf{E} = -\frac{\mathbf{v}}{c} \times \mathbf{B} , \quad (5)$$

can be combined (*e.g.*, Landau & Lifshitz 1960) to give the Helmholtz equation

$$\frac{d}{dt} \left(\frac{\mathbf{B}}{\rho} \right) = \left(\frac{\mathbf{B}}{\rho} \cdot \nabla \right) \mathbf{v} . \quad (6)$$

Here, \mathbf{E} is the electric field and c is the speed of light.

As \mathbf{l} is fixed to the flow, it satisfies the equation

$$\frac{d\mathbf{l}}{dt} = (\mathbf{l} \cdot \nabla) \mathbf{v} . \quad (7)$$

Comparing Eqs. (6) and (7) indicates that as (\mathbf{B}/ρ) and \mathbf{l} evolve, their ratio remains constant, such that

$$\mathbf{B} = \tilde{B} \frac{\rho \mathbf{l}}{\tilde{\rho} \tilde{l}} . \quad (8)$$

This equation holds for both steady and time-dependent flows, and even across surfaces of discontinuity. Using Eq. (8) to evolve \mathbf{B} from \tilde{H} guarantees that the MHD equations are satisfied everywhere, assuming continuity and that Gauss' law holds on \tilde{H} ; see Appendix A.

In our non-relativistic, ideal MHD limit, \mathbf{E} is small, and may be estimated from Eq. (5) once \mathbf{B} is known.

2.1.2. Lagrangian picture

For the subsequent analysis, it is useful to visualize the magnetic field amplitude as proportional to the density of field lines, *i.e.* inversely proportional to the distance ψ between them. Therefore, \mathbf{B} in the direction $\hat{\mathbf{l}}$ is inversely proportional to the perpendicular (to $\hat{\mathbf{l}}$) area element \mathcal{A} spanned by two such distances, ψ_1 and ψ_2 . Hence,

$$\mathbf{B} = \tilde{B} \frac{\tilde{\mathcal{A}}}{\mathcal{A}} \hat{\mathbf{l}} , \quad (9)$$

where $\mathcal{A} = \hat{\mathbf{l}} \cdot (\boldsymbol{\psi}_1 \times \boldsymbol{\psi}_2)$ is assumed infinitesimally small. As the mass $\rho \mathcal{A} l$ of the fluid element in the parallelogram spanned by $\{\mathbf{l}, \boldsymbol{\psi}_1, \boldsymbol{\psi}_2\}$ is constant, $\tilde{\mathcal{A}}/\mathcal{A} = \rho l / (\tilde{\rho} \tilde{l})$, and we recover Eq. (8).

2.2. Steady flow magnetization

2.2.1. General analysis

The flow can be fully determined by specifying two stream functions, λ_κ where $\kappa \in \{1, 2\}$ (henceforth), and an additional scalar field φ such as ρ , v , or Δt (Giese 1951). Two surfaces, defined by constant values of the stream functions, intersect along a streamline, so

$$\mathbf{v} \cdot \nabla \lambda_\kappa = 0 . \quad (10)$$

This equation, along with the time-independent continuity equation

$$\nabla \cdot (\rho \mathbf{v}) = 0 , \quad (11)$$

are identically satisfied by the λ gauge (Yih 1957)

$$\frac{\rho \mathbf{v}}{\tilde{\rho} \tilde{v}} = (\nabla \lambda_1 \times \nabla \lambda_2) = \begin{vmatrix} \hat{\mathbf{x}}_1 & \hat{\mathbf{x}}_2 & \hat{\mathbf{x}}_3 \\ \frac{\partial \lambda_1}{\partial x_1} & \frac{\partial \lambda_1}{\partial x_2} & \frac{\partial \lambda_1}{\partial x_3} \\ \frac{\partial \lambda_2}{\partial x_1} & \frac{\partial \lambda_2}{\partial x_2} & \frac{\partial \lambda_2}{\partial x_3} \end{vmatrix} , \quad (12)$$

where the second equality, as written without Lamé coefficients, holds only in Cartesian coordinates. For convenience, we take the stream functions in units of length, and so introduce the overall normalizations denoted by breve (henceforth; *e.g.*, $\rho/\tilde{\rho}$ is a dimensionless mass density). Equation (12) indicates that $\rho \mathbf{v}$ cannot be chosen as the independent φ , and that swapping λ_1 and λ_2 reverses the flow.

In order to parameterize the position of fluid elements in the volume spanned by the flow, we must introduce, in addition to λ_1 and λ_2 , a third variable $q(\mathbf{x})$, not necessarily equal to φ . The surfaces defined by λ_1 , λ_2 and q may never overlap; namely, the vectors

$$\mathbf{A}_1 = \nabla \lambda_1 ; \quad \mathbf{A}_2 = \nabla \lambda_2 ; \quad \mathbf{A}_3 = \left(\frac{v}{v_q} \right) \nabla q \quad (13)$$

should be coplanar throughout the flow. Here, $v_q \equiv dq/dt = \mathbf{v} \cdot \nabla q$ is the rate of change in q along the flow (in

units of q/t). The normalization factor (v/v_q) is included to keep the $\{\mathbf{A}_j\}$ basis dimensionless.

It is useful to introduce the reciprocal basis $\mathbf{a}_j = \mathbf{A}_j^{-1}$, defined (e.g., Kishan 2007) by $\mathbf{a}_i \cdot \mathbf{A}_j = \delta_{ij}$. Namely,

$$\mathbf{a}_1 \equiv \left(\frac{\partial \mathbf{x}}{\partial \lambda_1} \right)_q ; \mathbf{a}_2 \equiv \left(\frac{\partial \mathbf{x}}{\partial \lambda_2} \right)_q ; \mathbf{a}_3 \equiv \frac{v_q}{v} \left(\frac{\partial \mathbf{x}}{\partial q} \right)_{\tilde{\lambda}} = \hat{\mathbf{v}} . \quad (14)$$

Here, $\tilde{\lambda} \equiv \{\lambda_1, \lambda_2\}$, and it is understood (henceforth) that derivatives with respect to λ_1 (λ_2) are taken at a fixed λ_2 (λ_1). Like $\{\mathbf{A}_j\}$, the reciprocal basis too is dimensionless and coplanar. Note that the \mathbf{a}_j are not necessarily perpendicular to one another, and that the q -dependent $\mathbf{a}_{1,2}$ are not necessarily unit vectors.

An advantage of the $\{\mathbf{a}_j\}$ basis is that the $\kappa = \{1, 2\}$ components of any vector $\tilde{\mathbf{V}}$ in this basis are independent of q , as

$$\mathbf{V} = V_\kappa \mathbf{a}_\kappa + V_3 \mathbf{a}_3 = \begin{bmatrix} V_1 \\ V_2 \\ V_3 \end{bmatrix} = \begin{bmatrix} \mathbf{V} \cdot \mathbf{A}_1 \\ \mathbf{V} \cdot \mathbf{A}_2 \\ \mathbf{V} \cdot \mathbf{A}_3 \end{bmatrix} = \begin{bmatrix} \mathbf{V} \cdot \nabla \lambda_1 \\ \mathbf{V} \cdot \nabla \lambda_2 \\ \frac{v}{v_q} \mathbf{V} \cdot \nabla q \end{bmatrix} . \quad (15)$$

Moreover, for \mathbf{l} , the κ components l_κ are conserved along streamlines, as we show below. We use (henceforth) square brackets to denote vectors in the reciprocal basis, which in general is neither orthogonal nor normalized, and reserve round brackets for vectors in orthonormal bases.

Consider two infinitesimally close fluid elements, which at some instant are at the locations $\mathbf{x}(\lambda_\kappa, q)$ and

$$\begin{aligned} \mathbf{x} + \mathbf{l} &= \mathbf{x}(\lambda_\kappa + l_\kappa, q + \delta_q) \\ &= \mathbf{x}(\lambda_\kappa, q) + l_\kappa \left(\frac{\partial \mathbf{x}}{\partial \lambda_\kappa} \right)_q + \delta_q \left(\frac{\partial \mathbf{x}}{\partial q} \right)_{\tilde{\lambda}} + O(l^2) , \end{aligned} \quad (16)$$

where we generalized the Einstein summation rule also for stream function indices $\kappa = \{1, 2\}$ (and, later on, for path function indices $\alpha = \{1, 2, 3\}$). As $\tilde{\lambda}$ of each of the two fluid elements is conserved along the flow, the intervals $l_\kappa = \tilde{l}_\kappa$ are constant along the streamline.

Henceforth we work to first order in the infinitesimal l , which is then given by

$$\mathbf{l} = l_\kappa \mathbf{a}_\kappa + l_3 \mathbf{a}_3 = \tilde{l}_\kappa \mathbf{a}_\kappa + l_3 \mathbf{a}_3 = \begin{bmatrix} \tilde{l}_1 \\ \tilde{l}_2 \\ l_3 \end{bmatrix} , \quad (17)$$

where $l_3 = v \delta_q / v_q$. As $l_\kappa = \tilde{l}_\kappa$, the κ components of \mathbf{l} in the reciprocal basis are indeed seen to be constant along the streamline. In general, l_3 is not conserved. This decomposition is illustrated in Fig. 1.

In order to evaluate l_3 , consider the travel time Δt of a fluid element from \tilde{H} to the position \mathbf{x} ,

$$\Delta t(\mathbf{x}) = \int_{\tilde{q}(\mathbf{x})}^{q(\mathbf{x})} \frac{dq'}{v_q} . \quad (18)$$

During the same time, the $\mathbf{x} + \mathbf{l}$ fluid element travels

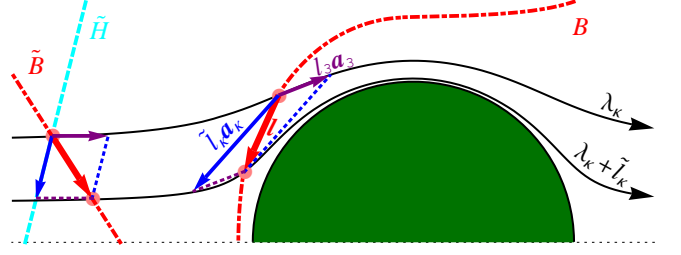


FIG. 1.— Evolution of an infinitesimal length element l (thick red arrows) between two fluid elements (pink disks), representing a field line element \mathbf{B} (dot-dashed red curves, with directionality given by l), illustrated at two different times for a flow around a blunt object (green half disk). The length element is decomposed (see Eq. 17) into components along ($l_3 \mathbf{a}_3$, purple arrows) the streamlines (thin black arrows) and along the stream function gradients ($l_\kappa \mathbf{a}_\kappa$, blue arrows; the latter are shown initially confined to the hypersurface \tilde{H} (dashed cyan curve), under the specific choice $q = \Delta t$; see §2.2.2).

from $\tilde{q} + \tilde{\delta}_q$ (not necessarily on \tilde{H}) to $q + \delta_q$, so

$$\int_{\tilde{q}}^q \frac{dq'}{v_q(\lambda_\kappa, q')} = \int_{\tilde{q} + \tilde{\delta}_q}^{q + \delta_q} \frac{dq'}{v_q(\lambda_\kappa + \tilde{l}_\kappa, q')} . \quad (19)$$

Expanding to first order in l indicates that

$$\frac{\delta_q}{v_q} = \frac{\tilde{\delta}_q}{\tilde{v}_q} - \tilde{l}_\kappa \frac{\partial \Delta t}{\partial \lambda_\kappa} , \quad (20)$$

where derivatives of $\Delta t = \Delta t(\tilde{\lambda}, q, \tilde{q})$ with respect to λ_κ are taken with the other arguments of Δt fixed. The component l_3 can now be related to the Lagrangian constants through

$$l_3 = v \frac{\delta_q}{v_q} = \tilde{l}_3 \frac{v}{\tilde{v}} - v \tilde{l}_\kappa \frac{\partial \Delta t}{\partial \lambda_\kappa} . \quad (21)$$

If a surface of constant q overlaps with one of the constant λ_κ surfaces, v_q vanishes and Eq. (20) is rendered invalid; a piecewise analysis may still be possible. The analysis breaks down at stagnation points, where Δt (and so also l and \mathbf{B}) diverges.

Finally, the length element \mathbf{l} is now given, throughout the flow connected to \tilde{H} , by

$$\mathbf{l} = \tilde{l}_\kappa \mathbf{a}_\kappa + \frac{v}{\tilde{v}} \left(\tilde{l}_3 - \tilde{l}_\kappa \tilde{v} \frac{\partial \Delta t}{\partial \lambda_\kappa} \right) = \begin{bmatrix} \tilde{l}_1 \\ \tilde{l}_2 \\ \frac{v}{\tilde{v}} \tilde{l}_3 \end{bmatrix} - \begin{bmatrix} 0 \\ 0 \\ v \end{bmatrix} \tilde{l}_\kappa \frac{\partial \Delta t}{\partial \lambda_\kappa} . \quad (22)$$

Note that in addition to \mathbf{a}_κ , the Δt derivative also depends on q . It can be written as

$$\frac{\partial \Delta t}{\partial \lambda_\kappa} \equiv \left(\frac{\partial \Delta t}{\partial \lambda_\kappa} \right)_{q, \tilde{q}} = - \int_{\tilde{q}}^q \frac{1}{v_q^2} \left(\frac{\partial v_q}{\partial \lambda_\kappa} \right)_{q'} dq' . \quad (23)$$

The Lagrangian constants are fixed at $\tilde{\mathbf{x}}$, where the streamline meets \tilde{H} . The point $\tilde{\mathbf{x}}(\mathbf{x})$ can be computed by inverting $\tilde{H}(\tilde{\mathbf{x}})$, as $\tilde{\lambda}(\mathbf{x}) = \tilde{\lambda}(\tilde{\mathbf{x}})$ is given, and remains constant along the streamline. The components \tilde{l}_j are found by projecting $\tilde{\mathbf{l}}$ onto the reciprocal basis as

in Eq. (15),

$$\tilde{l}_\kappa = \mathbf{l} \cdot \nabla \lambda_\kappa = (\mathbf{l} \cdot \nabla \lambda_\kappa)_{\tilde{H}} \quad \text{and} \quad \tilde{l}_3 = \left(\frac{v}{v_q} \mathbf{l} \cdot \nabla q \right)_{\tilde{H}}. \quad (24)$$

Equations (8) and (22) imply that

$$\mathbf{B} = \tilde{B} \frac{\rho \mathbf{l}}{\tilde{\rho} \tilde{l}} = \begin{bmatrix} \tilde{B}_1 \\ \tilde{B}_2 \\ \frac{v}{\tilde{v}} \tilde{B}_3 \end{bmatrix} \frac{\rho}{\tilde{\rho}} - \begin{bmatrix} 0 \\ 0 \\ \frac{\rho}{\tilde{\rho}} v \end{bmatrix} \tilde{B}_\kappa \frac{\partial \Delta t}{\partial \lambda_\kappa}, \quad (25)$$

where the Lagrangian constants $\tilde{B}_j = (\tilde{B}/\tilde{l})\tilde{l}_j$ are fixed by the projection Eq. (15) on \tilde{H} ,

$$\tilde{B}_\kappa = (\mathbf{B} \cdot \nabla \lambda_\kappa)_{\tilde{H}} \quad \text{and} \quad \tilde{B}_3 = \left(\frac{v}{v_q} \mathbf{B} \cdot \nabla q \right)_{\tilde{H}}. \quad (26)$$

Next, consider the electric field \mathbf{E} . The vector product $(\mathbf{v} \times \mathbf{B})$ in Eq. (5) eliminates all but the first term in Eq. (25), leaving

$$\mathbf{E} = \frac{\tilde{\rho} \tilde{v}}{\tilde{\rho} c} \left(\tilde{B}_2 \nabla \lambda_1 - \tilde{B}_1 \nabla \lambda_2 \right). \quad (27)$$

The electric field is therefore entirely determined by the stream functions, independent of φ , once \mathbf{B} and ρ are specified on \tilde{H} .

2.2.2. Choice of a third variable $q(\mathbf{x})$

There are various choices for the third variable q , depending on the specific problem at hand. A useful choice is the travel time Δt , which in some cases is easily estimated or computed. For $q = \Delta t$, which is the specific case illustrated in Fig. 1, Eqs. (22) and (25) reduce to

$$\mathbf{l} = \tilde{l}_\kappa \left(\frac{\partial \mathbf{x}}{\partial \lambda_\kappa} \right)_{\Delta t} + \tilde{l}_3 \frac{\mathbf{v}}{\tilde{v}} = \begin{bmatrix} \tilde{l}_1 \\ \tilde{l}_2 \\ \frac{v}{\tilde{v}} \tilde{l}_3 \end{bmatrix}, \quad (28)$$

and

$$\mathbf{B} = \left[\tilde{B}_\kappa \left(\frac{\partial \mathbf{x}}{\partial \lambda_\kappa} \right)_{\Delta t} + \tilde{B}_3 \frac{\mathbf{v}}{\tilde{v}} \right] \frac{\rho}{\tilde{\rho}} = \begin{bmatrix} \tilde{B}_1 \\ \tilde{B}_2 \\ \frac{v}{\tilde{v}} \tilde{B}_3 \end{bmatrix} \frac{\rho}{\tilde{\rho}}. \quad (29)$$

In the case of an irrotational flow, a potential Φ can be defined such that $\mathbf{v} = \tilde{v} \nabla \Phi$, where the normalization factor assigns Φ with units of length. Here we may choose $q = \Phi$, and read \mathbf{l} and \mathbf{B} off Eqs. (22) and (25), respectively, with the time derivative term (*cf.* Eq. 23)

$$\left(\frac{\partial \Delta t}{\partial \lambda_\kappa} \right)_{\Phi, \tilde{\Phi}} = -2\tilde{v} \int_{\tilde{\Phi}}^{\Phi} \frac{d\Phi'}{v^3} \left(\frac{\partial v}{\partial \lambda_\kappa} \right)_{\Phi'}. \quad (30)$$

Equipotential surfaces are perpendicular to the streamlines, so here \mathbf{a}_1 and \mathbf{a}_2 are conveniently perpendicular to \mathbf{a}_3 .

Among the infinite other possible choices of q , noteworthy are the natural coordinates of the flow, and the length $s(\mathbf{x})$ of the streamline from \tilde{H} to \mathbf{x} . In general, the simplest variable which is monotonic along the flow is preferable.

2.3. Time-dependent flow magnetization

A time-dependent flow can be fully specified by three path functions, $\Lambda_{\alpha=1,2,3}$ (Yih 1957). Three spacetime surfaces, defined by some constant values of these path functions, intersect along a pathline. Therefore, along the flow

$$\frac{d\Lambda_\alpha(\mathbf{x}, t)}{dt} = \left(\frac{\partial}{\partial t} + \mathbf{v} \cdot \nabla \right) \Lambda_\alpha(\mathbf{x}, t) = 0, \quad (31)$$

which determines \mathbf{v} through

$$\mathbf{v} = -\frac{\epsilon_{ijk} (\partial_t \Lambda_i) (\nabla \Lambda_j \times \nabla \Lambda_k)}{2(\nabla \Lambda_1 \times \nabla \Lambda_2) \cdot \nabla \Lambda_3}, \quad (32)$$

where ϵ_{ijk} is the Levi-Civita symbol. The continuity equation (3) is then identically satisfied by the Λ gauge (Yih 1957)

$$\frac{\rho}{\tilde{\rho}} = -(\nabla \Lambda_1 \times \nabla \Lambda_2) \cdot \nabla \Lambda_3. \quad (33)$$

For convenience, we take the path functions in units of length, and present Eqs. (32) and (33) as

$$\left(\frac{\rho}{\tilde{\rho}} \mathbf{v}, \frac{\rho}{\tilde{\rho}} \right) = \begin{bmatrix} \hat{\mathbf{x}}_1 & \hat{\mathbf{x}}_2 & \hat{\mathbf{x}}_3 & 1 \\ \frac{\partial \Lambda_1}{\partial x_1} & \frac{\partial \Lambda_1}{\partial x_2} & \frac{\partial \Lambda_1}{\partial x_3} & \frac{\partial \Lambda_1}{\partial t} \\ \frac{\partial \Lambda_2}{\partial x_1} & \frac{\partial \Lambda_2}{\partial x_2} & \frac{\partial \Lambda_2}{\partial x_3} & \frac{\partial \Lambda_2}{\partial t} \\ \frac{\partial \Lambda_3}{\partial x_1} & \frac{\partial \Lambda_3}{\partial x_2} & \frac{\partial \Lambda_3}{\partial x_3} & \frac{\partial \Lambda_3}{\partial t} \end{bmatrix}. \quad (34)$$

This expression, as written without Lamé coefficients, holds only in Cartesian coordinates.

To parameterize spacetime, we must introduce, in addition to Λ_1 , Λ_2 , and Λ_3 , also a fourth variable $Q(\mathbf{x}, t)$, provided that the hypersurfaces defined by these four parameters never overlap.

Define \mathbf{l} as the distance between two simultaneous, infinitesimally close spacetime events,

$$x^\mu(\Lambda_\alpha, Q) = \begin{pmatrix} t \\ \mathbf{x} \end{pmatrix} \quad (35)$$

and

$$\begin{pmatrix} t \\ \mathbf{x} + \mathbf{l} \end{pmatrix} = x^\mu + dx^\mu = x^\mu(\Lambda_\alpha + L_\alpha, Q + \delta_Q) \quad (36)$$

$$= x^\mu + L_\alpha \frac{\partial x^\mu}{\partial \Lambda_\alpha} + \delta_Q \frac{\partial x^\mu}{\partial Q},$$

where we defined $v_Q \equiv dQ/dt$ as the rate of change in Q along the flow (in units of Q/t), and work only to first order in l . As $x^\mu = x^\mu(\Lambda_\alpha, Q)$, derivatives with respect to Λ_α or Q are understood as taken with the other three arguments fixed. Here, the infinitesimal $L_\alpha = \tilde{L}_\alpha$, but not necessarily δ_Q , are constant along the pathline, because they are the differences between the conserved path function values.

The spacetime length element is now given by

$$\begin{pmatrix} 0 \\ \mathbf{l} \end{pmatrix} = \tilde{L}_\alpha \begin{pmatrix} \partial t / \partial \Lambda_\alpha \\ \partial \mathbf{x} / \partial \Lambda_\alpha \end{pmatrix} + \frac{\delta_Q}{v_Q} \begin{pmatrix} 1 \\ \mathbf{v} \end{pmatrix}. \quad (37)$$

The vanishing temporal component requires

$$\frac{\delta_Q}{v_Q} = -\tilde{L}_\alpha \frac{\partial t}{\partial \Lambda_\alpha}. \quad (38)$$

Therefore, the length element \mathbf{l} is given by

$$\mathbf{l} = \tilde{L}_\alpha \left(\frac{\partial \mathbf{x}}{\partial \Lambda_\alpha} - \mathbf{v} \frac{\partial t}{\partial \Lambda_\alpha} \right). \quad (39)$$

Equation (31) and the chain rule imply that the constant \tilde{L}_α satisfy

$$\tilde{L}_\alpha = \mathbf{l} \cdot \nabla \Lambda_\alpha = (\mathbf{l} \cdot \nabla \Lambda_\alpha)_{\tilde{H}} \quad (40)$$

all along a pathline, and are independent of Q . Equation (40) can therefore be evaluated on \tilde{H} , in order to find \tilde{L}_α .

Finally, according to Eqs. (8) and (39),

$$\mathbf{B} = \tilde{B}_\alpha \frac{\rho}{\tilde{\rho}} \left(\frac{\partial \mathbf{x}}{\partial \Lambda_\alpha} - \mathbf{v} \frac{\partial t}{\partial \Lambda_\alpha} \right), \quad (41)$$

where the Lagrangian constants $\tilde{B}_\alpha \equiv (\tilde{B}/\tilde{l})\tilde{L}_\alpha$ can be determined on \tilde{H} using

$$\tilde{B}_\alpha = (\mathbf{B} \cdot \nabla \Lambda_\alpha)_{\tilde{H}}. \quad (42)$$

As in the time-independent case, here too there is considerable freedom in choosing Q . A useful choice is the temporal coordinate, $Q = t$, for which Eqs. (39) and (41) reduce to

$$\mathbf{l} = \tilde{L}_\alpha \left(\frac{\partial \mathbf{x}}{\partial \Lambda_\alpha} \right)_t, \quad (43)$$

and

$$\mathbf{B} = \tilde{B}_\alpha \frac{\rho}{\tilde{\rho}} \left(\frac{\partial \mathbf{x}}{\partial \Lambda_\alpha} \right)_t. \quad (44)$$

Other choices of Q may be advantageous in certain circumstances.

The electric field in a time-dependent flow becomes

$$\mathbf{E} = \epsilon_{ijk} \frac{\tilde{\rho} \tilde{B}_i}{\tilde{\rho} c} \left(\frac{\partial \Lambda_j}{\partial t} \right) \nabla \Lambda_k. \quad (45)$$

2.4. Time-dependent description of a steady flow

To ascertain that §2.2 and §2.3 are mutually consistent, we consider an arbitrary steady flow, and regard it as time-dependent. If the steady flow is characterized by the stream functions λ_1 and λ_2 , we can set

$$\Lambda_1 = \lambda_1 \quad \text{and} \quad \Lambda_2 = \lambda_2. \quad (46)$$

Solving Eqs. (32) and (33) with the aid of Eq. (12) and the definitions of §2.2, we find that the third path function must be

$$\Lambda_3 = \check{v} (t - \Delta t). \quad (47)$$

The solution Eq. (43) for \mathbf{l} in the time dependent regime now gives

$$\begin{aligned} \mathbf{l} &= \tilde{l}_\kappa \left(\frac{\partial \mathbf{x}}{\partial \lambda_\kappa} \right)_{\Lambda_3, t} + \tilde{L}_3 \left(\frac{\partial \mathbf{x}}{\partial \Lambda_3} \right)_{\lambda_\kappa, t} \\ &= \tilde{l}_\kappa \left(\frac{\partial \mathbf{x}}{\partial \lambda_\kappa} \right)_{\Delta t} + \tilde{l}_3 \frac{\mathbf{v}}{\check{v}}, \end{aligned} \quad (48)$$

where we used Eqs. (24) and (40) to relate $(-\tilde{L}_3/\check{v}) = (\tilde{l}_3/\check{v})$. We have thus recovered the steady flow solution Eqs. (28), showing that the two formalisms, involving path and stream functions, are consistent when applied to steady flows.

With the above Λ_α , the time-dependent electric field in Eq. (45) reduces to the time-independent \mathbf{E} in Eq. (27).

3. STEADY AXISYMMETRIC FLOW MAGNETIZATION

3.1. General analysis in cylindrical coordinates

Consider a steady, axisymmetric flow. Using cylindrical coordinates $\{\varrho, \phi, z\}$, axisymmetric flows are characterized by $v_\phi = 0$, and by vanishing ϕ derivatives of the flow parameters. Therefore, constant ϕ surfaces are perpendicular to the flow, and we may choose $\lambda_1 \equiv \check{R}\phi$, where \check{R} is some arbitrary length scale of the problem. Since the velocity field \mathbf{v} is ϕ -independent, we may choose $\lambda_2 \equiv \lambda(\varrho, z)$. For these stream functions, Eq. (12) yields

$$\mathbf{v} = (v_\varrho, 0, v_z) = \frac{\check{\mu}}{\varrho \rho} \left(\frac{\partial \lambda}{\partial z}, 0, -\frac{\partial \lambda}{\partial \varrho} \right), \quad (49)$$

where $\boldsymbol{\mu} \equiv \rho \varrho \mathbf{v}$ is the ring mass flux, and has units of viscosity. Here, the normalizations \check{R} and $\check{\mu} \equiv \check{\rho} \check{v} \check{R}$ arise from our convention to assign stream functions with units of length.

In addition to λ_1 and λ_2 , we must now choose a third variable q to describe space. The choice $q = z$ is advantageous for simple flow regions in which v_z does not change sign. For our choice of stream functions and q , the reciprocal basis Eq. (14) becomes

$$\mathbf{a}_1 = \frac{\varrho}{\check{R}} \hat{\phi}; \quad \mathbf{a}_2 = -\frac{\check{\mu}}{\mu_z} \hat{\varrho}; \quad \mathbf{a}_3 = \hat{v}. \quad (50)$$

A given $\tilde{\mathbf{B}} = (\tilde{B}_\varrho, \tilde{B}_\phi, \tilde{B}_z)$ may now be decomposed as $\tilde{B}_i \tilde{\mathbf{a}}_i$, where (*cf.* Eq. 26)

$$\tilde{\mathbf{B}} = \begin{bmatrix} \tilde{B}_1 \\ \tilde{B}_2 \\ \tilde{B}_3 \end{bmatrix} = \begin{bmatrix} \tilde{B}_\phi \frac{\check{\mu}}{\varrho} \\ \check{\mu}_\varrho \tilde{B}_z - \check{\mu}_z \tilde{B}_\varrho \\ \tilde{B}_z \frac{\check{v}}{\check{v}_z} \end{bmatrix}. \quad (51)$$

Equation (25) now yields

$$\begin{aligned} \frac{\tilde{\rho}}{\rho} \mathbf{B} &= \frac{\varrho}{\check{R}} \tilde{B}_1 \hat{\phi} - \frac{\check{\mu}}{\mu_z} \tilde{B}_2 \hat{\varrho} + \frac{\mathbf{v}}{\check{v}} \left(\tilde{B}_3 - \tilde{B}_2 \check{v} \frac{\partial \Delta t}{\partial \lambda} \right) \\ &= \begin{pmatrix} \frac{\check{\mu}_z}{\mu_z} \tilde{B}_\varrho \\ \frac{\varrho}{\check{\rho}} \tilde{B}_\phi \end{pmatrix} + \begin{pmatrix} \frac{v_\varrho}{\check{v}_z} - \frac{\check{\mu}_\varrho}{\mu_z} \\ 0 \\ 0 \end{pmatrix} \tilde{B}_z - \begin{pmatrix} v_\varrho \\ 0 \\ v_z \end{pmatrix} \tilde{B}_2 \frac{\partial \Delta t}{\partial \lambda}. \end{aligned} \quad (52)$$

The only computation necessary is an integral for the time derivative term,

$$\frac{\partial \Delta t}{\partial \lambda} \equiv \left[\frac{\partial \Delta t(\varrho, z)}{\partial \lambda} \right]_{\phi, z, \check{z}} = - \int_{\check{z}}^z \frac{1}{v_z^2} \left(\frac{\partial v_z}{\partial \lambda} \right)_{\phi, z'} dz'. \quad (53)$$

Recall that vectors in round brackets are in an orthonormal (in the case of Eq. 52, cylindrical) basis, whereas vectors in square brackets (as in Eq. 51) are in the reciprocal basis.

The electric field is found from Eqs. (27), (49) and (51), and given simply by

$$\mathbf{E} = \frac{\tilde{v}}{c} \begin{pmatrix} -\frac{\mu_z}{\tilde{\mu}} \tilde{B}_\phi \\ \frac{\tilde{\rho}}{\tilde{\rho}} \frac{\tilde{\mu}_\phi \tilde{B}_z - \tilde{\mu}_z \tilde{B}_\phi}{\tilde{\mu}} \\ \frac{\mu_\phi}{\tilde{\mu}} \tilde{B}_\phi \end{pmatrix}. \quad (54)$$

3.2. The axis of symmetry

Next, we focus on the vicinity of the axis of symmetry, $\varrho = 0$, along which $v_\varrho = 0$. Taking the incident flow in the $(-\hat{z})$ direction, we denote the incoming velocity as $u(\rho \simeq 0, z) \equiv -v_z$, and assume it is finite. Then, Eq. (49) indicates that in the vicinity of the axis, $\lambda = f(z)\varrho^2 + O(\varrho^3)$, where $f(z) \equiv \rho u / (2\tilde{\mu})$. Along a streamline, λ is constant, therefore so is $\rho u \varrho^2$; this is a direct expression of mass conservation. In the vicinity of the axis, we may thus write $\varrho/\tilde{\varrho} = (\tilde{\rho}\tilde{u}/\rho u)^{1/2}$ along a streamline. This holds even in the presence of a shock, which conserves the normal, in this case axial, mass flux $j = \rho u$.

Equation (52) now becomes

$$\mathbf{B} = \begin{pmatrix} \frac{\rho}{\tilde{\rho}} \left(\frac{\tilde{z}}{j}\right)^{\frac{1}{2}} \tilde{B}_\varrho \\ \frac{\rho}{\tilde{\rho}} \left(\frac{\tilde{z}}{j}\right)^{\frac{1}{2}} \tilde{B}_\phi \\ \frac{j}{\tilde{\mu}} \tilde{B}_z \end{pmatrix} + C \begin{pmatrix} 0 \\ 0 \\ \tilde{B}_\varrho \end{pmatrix}, \quad (55)$$

where

$$C(z) \equiv -\frac{j\tilde{\mu}_z}{\tilde{\rho}\tilde{\mu}} \frac{\partial \Delta t}{\partial \lambda} = \frac{j\tilde{u}}{\sqrt{j}} \int_{\tilde{z}}^z \frac{u_1 dz'}{u_0^2 \sqrt{j}}, \quad (56)$$

and we expanded $u = u_0(z) + u_1(z)\rho + O(\rho^2)$.

For a potential flow, $u_1 = 0$, and so $C = 0$. Such a flow arises, for example, if a homogeneous incident flow remains subsonic or mildly supersonic (*e.g.*, Landau & Lifshitz 1959).

In order to find $\rho/\tilde{\rho}$, we approximate the plasma as a polytropic gas with an adiabatic index γ . The steady flow is governed, in addition to continuity, by Euler's equation,

$$(\mathbf{v} \cdot \nabla) \mathbf{v} = -\frac{\nabla P}{\rho} = -\frac{c_s^2 \nabla \rho}{\rho}, \quad (57)$$

and Bernoulli's equation,

$$\frac{u^2}{2} + \frac{c_s^2}{\gamma - 1} = \frac{\tilde{c}_s^2}{\gamma - 1} = \text{constant}. \quad (58)$$

Here, P is the fluid pressure, $c_s = (\gamma P/\rho)^{1/2}$ is the (local) speed of sound, and a bar denotes (henceforth) a putative stagnation point where $v = 0$, whether or not such a point lies along a given streamline.

The axial mass density solution is $\rho^2 \propto (S^2 - M_0^2)^{S^2}$, where $S \equiv [2/(\gamma - 1)]^{1/2}$, and $M_0 \equiv u/\tilde{c}_s$ is the axial Mach number with respect to the stagnation sound speed. Hence, away from shocks,

$$\frac{\rho}{\tilde{\rho}} = \left(\frac{S^2 - M_0^2}{S^2 - \tilde{M}_0^2} \right)^{1/(\gamma-1)} \quad (59)$$

can be used in Eq. (55) to find \mathbf{B} . When a shock is present, the Lagrangian constants here are taken downstream; if \tilde{H} is located upstream, the shock compression ratio $(\tilde{M}_0/W)^2$ should be incorporated. Here, $W \equiv [2/(\gamma + 1)]^{1/2}$ and S are the weak and strong shock limits of M_0 ; see Keshet & Naor (2014).

4. MAGNETIZATION OF BASIC FLOWS

To illustrate the solution of passive magnetization, derived in general in §2 and for axial symmetry in §3, here we study the magnetic fields evolving in specific basic flows. Steady, incompressible flows around a sphere are analyzed in the irrotational (and thus, effectively inviscid) case in §4.1, and in the viscous limit in §4.2. The magnetic amplification in front of a blunt object is considered §4.3. In §4.4 we study the simple, one-dimensional class of time-dependent flows.

4.1. Potential incompressible steady flow around a sphere

Consider the inviscid, incompressible, steady flow around a solid sphere. We assume that the incident flow is homogeneous, unidirectional, and subsonic, so the entire flow is irrotational. Here, the mass density $\rho = \tilde{\rho}$ is constant, the radius of the sphere is taken (henceforth) as $R = 1$, and the constant $\tilde{v} = -\tilde{u}\hat{z}$ is taken on \tilde{H} far upstream, $\tilde{z} \rightarrow \infty$. It is thus natural to choose $\tilde{\rho} = \tilde{\rho}$, $\tilde{R} = 1$ and $\tilde{v} = \tilde{u}$, so $\tilde{\mu} = \tilde{\rho}\tilde{u}$.

As $\nabla \cdot \mathbf{v} = 0$ and $\nabla \times \mathbf{v} = 0$, the flow satisfies the Poisson equation $\nabla^2 \Phi = 0$ for the velocity potential Φ , defined by $\mathbf{v} = \tilde{u} \nabla \Phi$. The solution for boundary conditions of a vanishing normal velocity across the sphere is

$$\Phi = -z \left(1 + \frac{1}{2r^3} \right). \quad (60)$$

Here we primarily use cylindrical coordinates, but occasionally allude to spherical coordinates $\{r, \theta, \phi\}$, where $r^2 = \varrho^2 + z^2$. Thus,

$$v_z = \tilde{u} \left(-1 - \frac{1}{2r^3} + \frac{3z^2}{2r^5} \right) \quad \text{and} \quad v_\varrho = \frac{3\tilde{u}\varrho z}{2r^5}. \quad (61)$$

The stream functions can be chosen as $\lambda_1 = \phi$ and, according to Eq. (49),

$$\lambda \equiv \lambda_2 = \frac{\varrho^2}{2} \left(1 - \frac{1}{r^3} \right), \quad (62)$$

such that $\tilde{\varrho} = (2\lambda)^{1/2}$.

Solving Euler's Eq. (57) gives the pressure

$$P = \tilde{P} + \tilde{\rho}\tilde{u}^2 \frac{4r^3 - 5 + 3(4r^3 - 1) \cos 2\theta}{16r^6}, \quad (63)$$

where $\cos 2\theta = (z^2 - \varrho^2)/r^2$. Note that an incident pressure smaller than $(5/8)\tilde{\rho}\tilde{u}^2$ would lead to a nonphysical $P < 0$ around $z = 0$, as the plasma would be too cold to remain incompressible.

4.1.1. The natural choice $q = z$

For the choice $q = z$, which is natural because z monotonically decreases for all fluid elements, the magnetic

field is given by (cf. Eq. 52)

$$\mathbf{B} = \tilde{B}_\phi \frac{\tilde{\varrho}}{\varrho} \hat{\phi} - \tilde{B}_\varrho \frac{\tilde{\varrho}\tilde{u}}{\varrho v_z} \hat{\varrho} - \frac{\mathbf{v}}{\tilde{u}} \left(\tilde{B}_z - \tilde{B}_\varrho \tilde{\varrho} \tilde{u} \frac{\partial \Delta t}{\partial \lambda} \right), \quad (64)$$

where

$$\frac{\partial \Delta t}{\partial \lambda} \equiv \left(\frac{\partial \Delta t}{\partial \lambda} \right)_{\phi, z, \tilde{z}} = -\frac{12}{\tilde{u}} \int_{-\infty}^z \frac{r'^8 (r'^2 - 5z'^2) dz'}{(r'^2 + 2r'^5 - 3z'^2)^3}. \quad (65)$$

The integral is taken at a constant λ , so r' depends on z' through Eq. (62).

Figure 2 shows a constant ϕ slice through the flow, depicting the pressure (grayscale) and the magnetic field components initially parallel (colorscaled arrows) or perpendicular (colorscaled curves) to the velocity. For illustrative purposes, in the figure we take $\tilde{P} = \tilde{\rho}\tilde{u}^2$.

4.1.2. The problematic choice $q = r$

Another seemingly possible choice is $q = r$. According to Eq. (25), the magnetic field may then be written as

$$\mathbf{B} = \tilde{B}_\phi \frac{\tilde{\varrho}}{\varrho} \hat{\phi} + \tilde{B}_\varrho \frac{\varrho r}{\tilde{\varrho} z} \hat{\theta} - \frac{\mathbf{v}}{\tilde{u}} \left(\tilde{B}_z - \tilde{B}_\varrho \tilde{\varrho} \tilde{u} \frac{\partial \Delta t}{\partial \lambda} \right), \quad (66)$$

where

$$\frac{\partial \Delta t}{\partial \lambda} \equiv \left(\frac{\partial \Delta t}{\partial \lambda} \right)_{\phi, r, \tilde{r}} = \int_{-\infty}^r \frac{-r'^4 dr' / \tilde{u}}{(r'^3 - 1)^2 \left(1 - \frac{2\lambda r'}{r'^3 - 1} \right)^{\frac{3}{2}}}. \quad (67)$$

However, this result, obtained previously (Dursi & Pfrommer 2008; Romanelli et al. 2014) by solving the MHD equations, is strictly valid only in the half space $\theta < \pi/2$. At the surface $\theta = \pi/2$, the denominator of the integrand diverges, and the integration cannot be continued. This is to be expected, as surfaces of constant λ and surfaces of constant q overlap at $\theta = \pi/2$, as ∂_λ and ∂_r become parallel.

The integral in Eq. (67) can be solved analytically as a power series in λ ; see appendix B.

4.1.3. The orthogonal choice $q = \Phi$

Another optional choice for q is the velocity potential Φ . Here, the reciprocal basis becomes

$$\mathbf{a}_1 = \varrho \hat{\phi}; \quad \mathbf{a}_2 = \frac{(-v_z, 0, v_\varrho)}{\tilde{u} \varrho \left[\frac{\Phi^2}{z^2} - \frac{3z^2}{r^5} \left(1 - \frac{1}{4r^3} \right) \right]}; \quad \mathbf{a}_3 = \hat{\nu}, \quad (68)$$

are perpendicular to one another, and therefore may be useful as an orthogonal (albeit not orthonormal) basis. The magnetic field is then given by

$$\mathbf{B} = \begin{bmatrix} \tilde{\varrho}^{-1} \tilde{B}_\phi \\ -\tilde{\varrho} \tilde{B}_\varrho \\ \frac{v}{\tilde{u}} \tilde{B}_z \end{bmatrix} + \begin{bmatrix} 0 \\ 0 \\ \tilde{\varrho} v \end{bmatrix} \tilde{B}_\varrho \frac{\partial \Delta t}{\partial \lambda} \quad (69)$$

(in the $\{\mathbf{a}_j\}$ basis), and

$$\begin{aligned} \frac{\partial \Delta t}{\partial \lambda} &\equiv \left(\frac{\partial \Delta t}{\partial \lambda} \right)_{\phi, \Phi, \tilde{\Phi}} \\ &= \frac{48}{\tilde{u}} \int_{-\infty}^{\Phi} \frac{z'^4 r' + 4r'^9 \Phi'^2 + 10z'^4 r'^3 (1 - 2r'^4)}{4r'^8 \Phi'^2 + 3z'^4 (1 - 4r'^3)} d\Phi'. \end{aligned} \quad (70)$$

The parameters $r'(\Phi', \lambda)$ and $z'(\Phi', \lambda)$ are found from Eqs. (60) and (62), as the integral is taken at a constant λ .

4.2. Stokes (creeping) incompressible steady flow around a sphere

Consider the Stokes, incompressible, steady flow around a solid sphere. As in §4.1, $\rho = \tilde{\rho}$ is constant, the radius of the sphere is taken as $R = 1$, we assume that the incident flow $\tilde{\mathbf{v}} \equiv -\tilde{u}\hat{z}$, taken on \tilde{H} far upstream ($\tilde{z} \rightarrow \infty$), is homogeneous and unidirectional, and use a mixture of cylindrical and spherical coordinates. It is again natural to choose $\check{\rho} = \tilde{\rho}$, $\check{R} = 1$ and $\check{v} = \tilde{u}$, so $\check{\mu} = \tilde{\rho}\tilde{u}$.

Stokes flows are characterized by viscous forces that are much greater than the inertial forces, therefore the flow is governed by the approximate Navier-Stokes equation

$$0 = -\nabla \left(\frac{P}{\tilde{\rho}} \right) + \nu \nabla^2 \mathbf{v}, \quad (71)$$

where ν is the kinematic viscosity, assumed constant. Taking the curl of this equation gives

$$\nabla \times (\nabla^2 \mathbf{v}) = 0. \quad (72)$$

The solution for the boundary conditions of a hard sphere is

$$v_z = -\tilde{u} \left(1 - \frac{1}{r} \right) \left[1 + \frac{(r^2 - 3z^2)(r+1)}{4r^4} \right], \quad (73)$$

and

$$v_\varrho = 3\tilde{u} \left(1 - \frac{1}{r^2} \right) \frac{\varrho z}{4r^3}. \quad (74)$$

Solving Eq. (71) gives the pressure distribution

$$P = \tilde{P} + \tilde{\rho}\tilde{u}\nu \frac{3z}{2r^3}. \quad (75)$$

Here too, the incident plasma cannot be too cold, as an incident pressure $\tilde{P} < (3/2)\tilde{\rho}\tilde{u}^2/Re$, where $Re = \tilde{u}R/\nu$ is the incident Reynolds number, would lead to a non-physical $P < 0$ around the $z < 0$ axis.

The stream functions can be chosen as $\lambda_1 = \phi$ and, according to Eq. (49),

$$\lambda \equiv \lambda_2 = \frac{\varrho^2}{2} \left(1 - \frac{1}{r} \right)^2 \left(1 + \frac{1}{2r} \right), \quad (76)$$

such that $\tilde{\varrho} = (2\lambda)^{1/2}$. For the natural choice $q = z$, the magnetic field is given by

$$\mathbf{B} = \tilde{B}_\phi \frac{\tilde{\varrho}}{\varrho} \hat{\phi} - \tilde{B}_\varrho \frac{\tilde{\varrho}\tilde{u}}{\varrho v_z} \hat{\varrho} - \frac{\mathbf{v}}{\tilde{u}} \left(\tilde{B}_z - \tilde{B}_\varrho \tilde{\varrho} \tilde{u} \frac{\partial \Delta t}{\partial \lambda} \right), \quad (77)$$

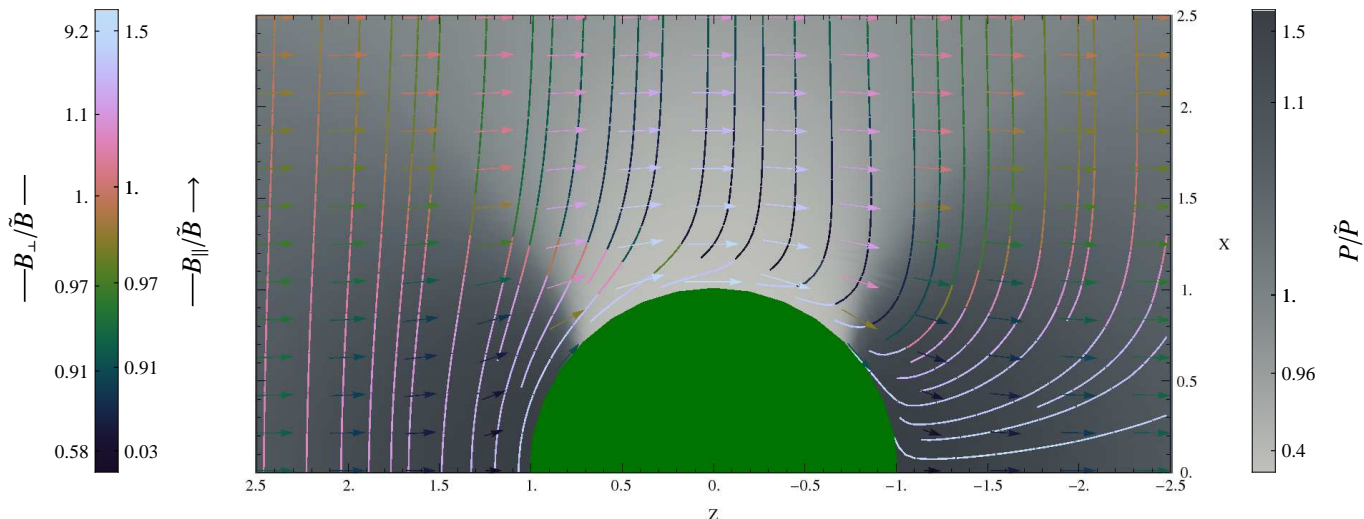


FIG. 2.— Potential incompressible steady flow around a solid sphere (green half disk), for a uniform magnetic field far upstream. The constant ϕ slice shows the pressure enhancement (gray scale; for $\tilde{P} = \tilde{\rho}\tilde{u}^2$) and the magnetic amplification B/\tilde{B} (colorscale; Green 2011) for field lines initially parallel (arrows) or perpendicular (solid curves) to the flow.

which is formally equivalent to Eq. (64). Here,

$$\begin{aligned} \frac{\partial \Delta t}{\partial \lambda} &\equiv \left(\frac{\partial \Delta t}{\partial \lambda} \right)_{\phi, z, \tilde{z}} \\ &= \frac{48}{\tilde{u}} \int_{\infty}^z \frac{r'^6 - 5z'^2 r'^2 + r'^4 (1 + 3z'^2)}{\left(1 - \frac{1}{r'^2}\right)^3 \left(r'^2 - 3z'^2 + \frac{4r'^4}{1+r'}\right)^3} dz'. \end{aligned} \quad (78)$$

The integral is taken at a constant λ , so r' depends on z' through Eq. (76).

Figure 3 shows the pressure and magnetization in such a flow, with the same notations used in Fig. 2. For illustrative purposes, in the figure $\tilde{P} = \tilde{\rho}\tilde{u}^2/Re$.

4.3. Magnetic layers

Under our assumptions, as the flow approaches the stagnation point in front of an object, the magnetic field initially perpendicular to the flow diverges, as seen in Figs. 2 and 3. The divergence here, around the object, and in the wake behind it, may be regarded as due to the pileup of infinitely many field lines, continuously stretched around the object, eventually wrapped closely around it and stretching to infinity along the wake.

These nonphysical divergencies signal the breakdown of our assumptions in the above regions. In particular, the magnetic field here can no longer be regarded as dynamically insignificant, and eventually resistivity can no longer be neglected (*e.g.*, Chacko & Hassam 1997; Lyutikov 2006).

It is useful to consider the extent of the highly magnetized layer forming in front of an object in an arbitrary axisymmetric flow. Define the magnetic pressure fraction

$$\epsilon_B \equiv \beta_p^{-1} = \frac{B^2/4\pi}{P_T}, \quad (79)$$

where β_p is the beta of the plasma, and P_T is the thermal pressure. The fractional magnetic amplification may then be defined as

$$\frac{\epsilon_B}{\tilde{\epsilon}_B} = \left(\frac{B}{\tilde{B}} \right)^2 \left(\frac{P_T}{\tilde{P}_T} \right)^{-1}. \quad (80)$$

Figure 4 shows the amplifications of magnetic pressure $\sim B^2$ and pressure fraction ϵ_B as a function of the distance $\delta \equiv r - 1$ in front of the unit sphere, for various steady flows: an incompressible potential flow, a Stokes incompressible flow, and inviscid compressible flows in the subsonic and mildly supersonic regimes. As the above flows are approximately (for the mildly supersonic case), or precisely, irrotational along the axis, Eqs. (55) and (56) become

$$B(z)^2 = \tilde{B}_{\perp}^2 \frac{\tilde{j}\rho^2}{j\tilde{\rho}^2} + \tilde{B}_{\parallel}^2 \frac{j^2}{\tilde{j}^2}, \quad (81)$$

where \tilde{B}_{\perp} and \tilde{B}_{\parallel} are the axial magnetic field components initially perpendicular and parallel to the flow.

As Fig. 4 shows, viscosity induces magnetic amplification farther from the body. Compressibility has a similar, but somewhat weaker, effect on magnetization, but the magnetic pressure fraction is not strongly affected; the large difference in ϵ_B between the incompressible and compressible inviscid flows arises from the different pressure profiles due to the different equations of state.

Close to stagnation, the flow is adiabatic, ρ and P_T approach constant values, and \mathbf{B} becomes primarily transverse, so

$$\epsilon_B \propto \frac{B_{\perp}^2}{P_T} \propto B_{\perp}^2 \propto \frac{\rho^2}{j} \propto v^{-1}, \quad (82)$$

which scales as δ^{-2} for the Stokes flow, and as δ^{-1} for the incompressible potential flow; the latter approximately characterizes the stagnation region even for compressible flows, except in the highly supersonic regime.

The passive magnetization assumption eventually fails, at some level of magnetic amplification which depends on the initial magnetization $\tilde{\epsilon}_B$. The corresponding width of the magnetized region is crudely given, according to Eq. (82), by

$$\delta \sim \begin{cases} \tilde{\epsilon}_B^{-1} & \text{for negligible viscosity;} \\ \tilde{\epsilon}_B^{-1/2} & \text{for strong viscosity.} \end{cases} \quad (83)$$

For the compressible flows, we use the approximate

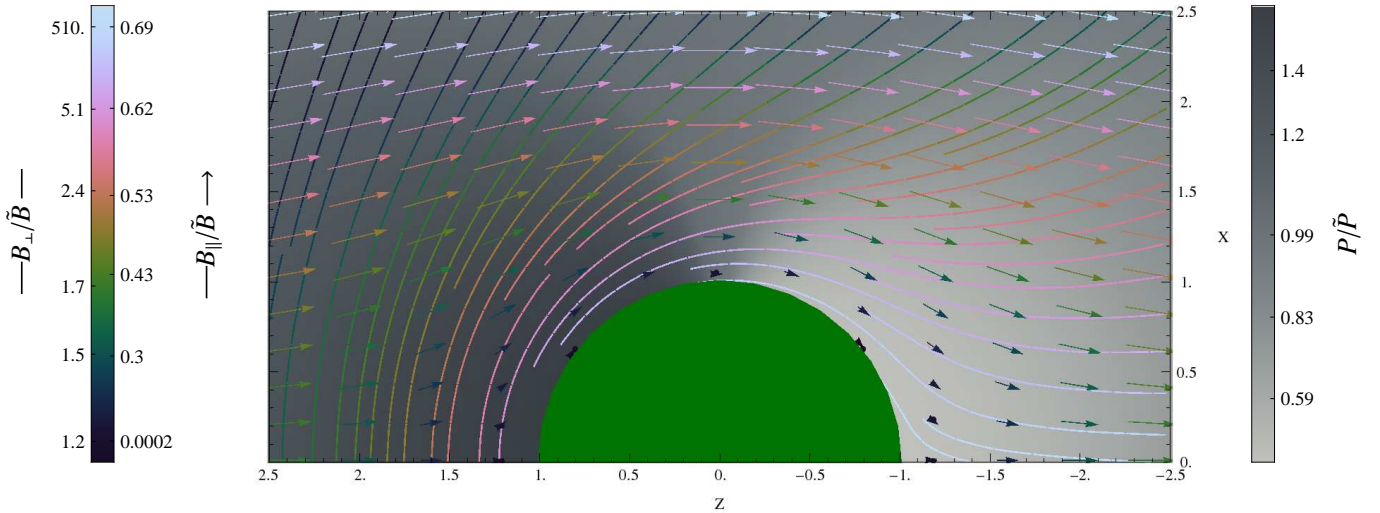


FIG. 3.— Stokes incompressible steady flow around a solid sphere. Notations are as in Fig. 2, with $\tilde{P} = \tilde{\rho} \tilde{u}^2 / Re$.

solutions of Keshet & Naor (2014, using $\gamma = 5/3$ and $\beta = 0.52$). In the supersonic regime, \tilde{H} is assumed to be upstream, so the jumps in B_\perp and P_T across the shock are taken into account. Here, the flow remains nonmagnetized until reaching the shock, at the so called stand-off distance $\delta = \Delta$; for high \tilde{M}_0 , the magnetized layer slightly shrinks as Δ diminishes.

4.4. One dimensional, time dependent flow

As a simple illustration of magnetization in the time-dependent regime, consider the case of an arbitrary one-dimensional flow. Classical examples include the plasma in a cylindrical pipe, disturbed by a moving piston, or a one-dimensional rarefaction wave. If discontinuities are present in the flow, the following applies separately to each region bounded by surfaces of discontinuity or \tilde{H} .

Without loss of generality, take the flow in the \hat{x} direction, such that $\mathbf{v} = v\hat{x}$ and the perpendicular velocity components vanish. A simple choice of path functions is then

$$\Lambda_2 = y \quad \text{and} \quad \Lambda_3 = z, \quad (84)$$

as both are constant along the flow. Equations (32) and (33) then constrain Λ_1 , as

$$\left(\frac{\partial \Lambda_1}{\partial x} \right)_{y,z,t} = -\frac{\rho}{\tilde{\rho}} \quad \text{and} \quad \left(\frac{\partial \Lambda_1}{\partial t} \right)_{x,y,z} = \frac{\rho v}{\tilde{\rho}}. \quad (85)$$

The solution is the path function family

$$\Lambda_1(x) = -\frac{1}{\tilde{\rho}} \int^x \rho dx' + C, \quad (86)$$

where we used the continuity equation, and C is a constant with no further significance.

For a given $\tilde{\mathbf{l}} = (\tilde{l}_x, \tilde{l}_y, \tilde{l}_z)$, Eq. (40) yields the Lagrangian constants

$$\tilde{L}_1 = -\frac{\tilde{\rho}}{\rho} \tilde{l}_x; \quad \tilde{L}_2 = \tilde{l}_y; \quad \tilde{L}_3 = \tilde{l}_z. \quad (87)$$

Equivalently, for $\tilde{\mathbf{B}} = (\tilde{B}_x, \tilde{B}_y, \tilde{B}_z)$,

$$\tilde{B}_1 = -\frac{\tilde{\rho}}{\rho} \tilde{B}_x; \quad \tilde{B}_2 = \tilde{B}_y; \quad \tilde{B}_3 = \tilde{B}_z. \quad (88)$$

Finally, Eqs. (43) and (44) give, respectively

$$\mathbf{l} = \left(\frac{\tilde{\rho}}{\rho} \tilde{l}_x, \tilde{l}_y, \tilde{l}_z \right), \quad (89)$$

and

$$\mathbf{B} = \left(\tilde{B}_x, \frac{\rho}{\tilde{\rho}} \tilde{B}_y, \frac{\rho}{\tilde{\rho}} \tilde{B}_z \right). \quad (90)$$

Equations (89) and (90) can be seen directly from Lagrangian considerations. Since the gas flows only in the x direction, the perpendicular (to the flow) distance between fluid elements is constant. Perpendicular length elements $\{l_y, l_z\}$ and the parallel magnetic field B_x , are thus conserved. The parallel distance between nearby fluid elements is simply $l_x \propto \rho^{-1}$, so the perpendicular fields follow $\{B_y, B_z\} \propto \rho$.

5. SUMMARY AND DISCUSSION

We have shown that stream functions and path functions, often used to describe non-diffusive flows, provide a simple, local solution to the problem of evolving electromagnetic fields in a highly conductive plasma. Equivalently, they locally fix the evolution of a length element \mathbf{l} embedded in the flow. Expressions were provided, in both steady and time-dependent flows, for the evolution of the magnetic field \mathbf{B} (Eqs. 29 and 44), the electric field \mathbf{E} (Eqs. 27 and 45), and \mathbf{l} (Eqs. 28 and 43).

The analysis is illustrated in Fig. 1 for a steady flow. Its results are manifestly local, and thus conceptually simpler and more general than previous solutions of the ideal MHD equations. It is valid for arbitrary flows continuously connected to some hypersurface \tilde{H} where \mathbf{B} is known, even in the presence of discontinuities.

The generality of the analysis allows us to quickly reproduce known solutions such as for a potential incompressible flow around a sphere (Eqs. 66 and Fig. 2), and to derive new solutions for magnetization in various flows such as an arbitrary axially symmetric flow (Eq. 52), the

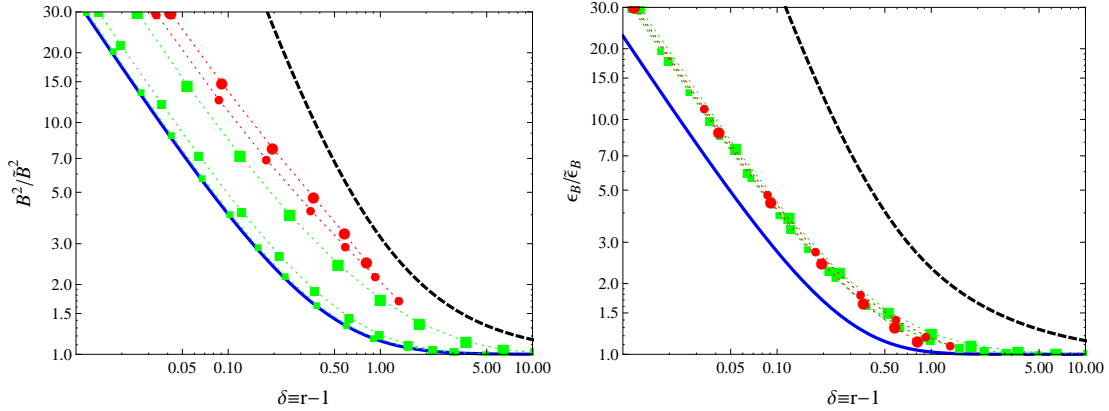


FIG. 4.— Head on ($\theta = 0$) amplification of the magnetic pressure (left) and magnetic pressure fraction (right), plotted against the distance δ from the nose of the unit sphere, for various steady flows: incompressible potential (solid blue; for $\tilde{P} = \tilde{\rho}v^2$), Stokes incompressible (dashed black; for $\tilde{P} = \tilde{\rho}v^2/Re$), and inviscid compressible (symbols with dotted lines to guide the eye) in the subsonic ($\tilde{M} \in \{0.2, 0.5, 0.95\}$); green squares, small to large) and mildly supersonic ($\tilde{M} \in \{1.2, 1.4\}$); red circles, small to large) regimes.

incompressible Stokes flow around a sphere (Eqs. 77 and Fig. 3) and the compressible flow in front of a blunt axisymmetric object (Eq. 81 and Fig. 4).

For steady flows, a third variable q is needed, in addition to the two stream functions, in order to map the volume spanned by the flow. Our analysis utilizes the freedom in the choice of this q ; see Eqs. (22) and (25). Computing the evolution of \mathbf{B} becomes particularly simple for certain choices of q , in particular if the travel time parameter Δt is measured or easily computed; other choices require, in general, one integration (Eq. 23). Conveniently, the evolution of \mathbf{E} is entirely fixed by the stream functions alone, given boundary conditions on \tilde{H} .

For time-dependent flows, the analysis is conceptually simpler because the three path functions entirely determine the flow; the freedom in the choice of a fourth variable Q is less important. Here, no integration is necessary when Λ_α are known. The analysis is demonstrated for an arbitrary one dimensional flow (Eqs. 89 and 90).

The magnetization in front of an axisymmetric blunt object (Eq. 55) simplifies considerably if the flow along the axis is approximately irrotational (as C in Eq. 56 vanishes). The simple relation thus obtained between B and v can be used to directly infer one quantity, if the other is known. Here, the magnetic pressure (Eq. 81)

and magnetic pressure fraction (Eq. 80) increase towards the stagnation point, roughly as v^{-1} (see Eq. 82), as illustrated for various flows in Fig. 4.

Viscosity and compressibility are seen to enhance the magnetization, leading to a thicker magnetized layer. However, the magnetic pressure fraction is apparently insensitive to compressibility. Crudely, the thickness of the magnetic layer depends on the upstream magnetization through Eq. (83).

Our approach directly links the properties of electromagnetic fields to the properties of path functions and stream functions. This connection, as far as we know unexplored so far, may thus help shed light on both sides. Even if only one stream function is (or only 1–2 path functions are) known, our approach may still provide valuable constraints on the electromagnetic field evolution. Vice versa, if the electromagnetic fields are known, the stream (or path) functions may be constrained, or even determined.

This research was funded by the European Union Seventh Framework Programme (FP7/2007-2013) under grant agreement n° 293975, an IAEC-UPBC joint research foundation grant 257/14, and an ISF-UGC grant.

APPENDIX

A. THE RELATION $\mathbf{B} \propto \rho \mathbf{v}$ PRESERVES THE MHD EQUATIONS

We evolve the electromagnetic fields using Eq. (8), or equivalently the Helmholtz equation (6), so it is useful to explicitly prove that the resulting \mathbf{B} satisfies Gauss' law (2) and the convection equation (4). We assume that the Helmholtz equation and the continuity equation (3) are satisfied everywhere, and that Gauss' law is satisfied on \tilde{H} .

First note that

$$\frac{\partial \mathbf{B}}{\partial t} - \nabla \times (\mathbf{v} \times \mathbf{B}) = \frac{\partial \mathbf{B}}{\partial t} - (\mathbf{B} \cdot \nabla) \mathbf{v} + (\mathbf{v} \cdot \nabla) \mathbf{B} + \mathbf{B} (\nabla \cdot \mathbf{v}) - \mathbf{v} (\nabla \cdot \mathbf{B}) = (-\mathbf{v}) (\nabla \cdot \mathbf{B}) , \quad (\text{A1})$$

where we used the Helmholtz and continuity equations in the last equality. This ensures that if Gauss' law is satisfied, then the convection equation (4) is guaranteed, and vice versa.

Taking the divergence of this equation yields

$$\frac{d(\nabla \cdot \mathbf{B})}{dt} = -(\nabla \cdot \mathbf{v}) (\nabla \cdot \mathbf{B}) . \quad (\text{A2})$$

Now, starting from \tilde{H} , we have

$$(\nabla \cdot \mathbf{B})_{\tilde{t}+dt} \simeq (\nabla \cdot \mathbf{B})_{\tilde{t}} + dt \left[\frac{d(\nabla \cdot \mathbf{B})}{dt} \right]_{\tilde{t}} = dt \left[\frac{d(\nabla \cdot \mathbf{B})}{dt} \right]_{\tilde{t}} = -dt (\nabla \cdot \mathbf{v})_{\tilde{t}} (\nabla \cdot \mathbf{B})_{\tilde{t}} = 0. \quad (\text{A3})$$

This result can be iteratively repeated, to cover the entire flow connected to \tilde{H} .

B. THE INTEGRAL $(\partial_\lambda \Delta t)_r$ FOR A STEADY INCOMPRESSIBLE POTENTIAL FLOW AROUND A SPHERE

The integral in Eq. (67) can be solved by expanding the integrand about $\lambda = 0$. This expansion is useful for analyzing the flow in the close vicinity of the axis of symmetry or of the sphere, where λ is small. The result is

$$\int \frac{r^4 dr}{(r^3 - 1)^2 \left(1 - \frac{2\lambda r}{r^3 - 1}\right)^{\frac{3}{2}}} = \sum_{n=0}^{\infty} b_n(r) (2\lambda)^n, \quad (\text{B1})$$

where n is an integer,

$$b_n(r) = \frac{2\Gamma\left(n + \frac{3}{2}\right) (-1)^n r^{n+2}}{n!(n+2)\sqrt{\pi}} \left[{}_2F_1\left(\frac{2+n}{3}, 2+n; \frac{5+n}{3}; r^3\right) - {}_2F_1\left(1+n, \frac{2+n}{3}; \frac{5+n}{3}; r^3\right) \right], \quad (\text{B2})$$

Γ is the Euler Gamma function, and ${}_2F_1$ is the hypergeometric function. In particular,

$$b_0 = \frac{1}{9} \left\{ 2\sqrt{3} \arctan\left(\frac{1+2r}{\sqrt{3}}\right) + \log\left[\frac{(r-1)^2}{1+r+r^2}\right] - \frac{3r^2}{r^3-1} \right\}, \quad \text{and} \quad b_1 = \frac{1-2r^3}{4(r^3-1)^2}. \quad (\text{B3})$$

REFERENCES

- Aleksashov, D. B., Baranov, V. B., Barsky, E. V., & Myasnikov, A. V. 2000, *Astronomy Letters*, 26, 743
- Bennett, J. S. 2008, Cranfield: Cranfield University.
- Bernikov, L. V., & Semenov, V. S. 1979, *Geomagnetism and Aeronomy*, 19, 671
- Brüggen, M. 2013, *Astronomische Nachrichten*, 334, 543
- Chacko, Z., & Hassam, A. B. 1997, *Physics of Plasmas*, 4, 3031
- Corona-Romero, P., & Gonzalez-Esparza, A. 2013, *Advances in Space Research*, 51, 1813
- Dursi, L. J., & Pfrommer, C. 2008, *ApJ*, 677, 993, 0711.0213
- Elsasser, W. M. 1956, *Reviews of Modern Physics*, 28, 135
- Giese, J. H. 1951, *J. Math. Phys.*, 30, 31
- Green, D. A. 2011, *Bulletin of the Astronomical Society of India*, 39, 289, 1108.5083
- Keshet, U., Markevitch, M., Birnboim, Y., & Loeb, A. 2010, *ApJ*, 719, L74, 0912.3526
- Keshet, U., & Naor, Y. 2014
- Kim, K.-T., Tribble, P. C., & Kronberg, P. P. 1991, *ApJ*, 379, 80
- Kishan, H. 2007, *Vector Algebra and Calculus*
- Landau, L. D., & Lifshitz, E. M. 1959, *Fluid mechanics*
- . 1960, *Electrodynamics of continuous media*
- Leal, L. G. 2007, *Advanced Transport Phenomena*
- Li, H.-B., Blundell, R., Hedden, A., Kawamura, J., Paine, S., & Tong, E. 2011, *MNRAS*, 411, 2067, 1007.3312
- Longcope, D. W. 2005, *Living Reviews in Solar Physics*, 2, 7
- Lyutikov, M. 2006, *MNRAS*, 373, 73, astro-ph/0604178
- Padovani, M., Galli, D., Hennebelle, P., Commerçon, B., & Joos, M. 2014, *A&A*, 571, A33, 1408.5901
- Parker, E. N. 1961, *ApJ*, 134, 20
- Price, D. J., & Bate, M. R. 2008, *MNRAS*, 385, 1820, 0801.3293
- Ranger, K. B. 1997, *Physics of Plasmas*, 4, 566
- Röken, C., Kleimann, J., & Fichtner, H. 2014, *ArXiv e-prints*, 1412.7199
- Romanelli, N., Gómez, D., Bertucci, C., & Delva, M. 2014, *ApJ*, 789, 43, 1406.4779
- Sekhar, T. V. S. 2003, *Computational Mechanics*, 31, 437
- Sekhar, T. V. S., Sivakumar, R., & Ravi Kumar, T. V. R. 2005, *Fluid Dynamics Research*, 37, 357
- Spreiter, J. R., & Alksne, A. Y. 1970, *Annual Review of Fluid Mechanics*, 2, 313
- Spreiter, J. R., & Stahara, S. S. 1995, *Advances in Space Research*, 15, 433
- Vallée, J. P. 2011, *New A Rev.*, 55, 91
- Vikhlinin, A., Markevitch, M., & Murray, S. S. 2001, *ApJ*, 549, L47, astro-ph/0008499
- Whang, Y. C. 2010, *ApJ*, 710, 936
- Widrow, L. M. 2002, *Reviews of Modern Physics*, 74, 775, astro-ph/0207240
- Yih, C. S. 1957, *La Houille Blanche*, 3, 445
- Zhang, M., & Low, B. C. 2005, *ARA&A*, 43, 103
- Zhang, T. L., Khurana, K. K., Russell, C. T., Kivelson, M. G., Nakamura, R., & Baumjohann, W. 2004, *Advances in Space Research*, 33, 1920